THREE-DIMENSIONAL CHARACTERIZATION OF STRUCTURE AND DAMAGE OF POLYMERS USING A TALBOT-LAU GRATING INTERFEROMETER µ-XCT

J. Kastner[1], S. Senck[1], B. Plank[1], D. Salaberger[1], G. Rao[1], and C. Gusenbauer[1]

[1]University of Applied Sciences Upper Austria, Austria
Email: johann.kastner@fh-wels.at, Web Page: http://www.fh-ooe.at

Keywords: X-ray computed tomography, damage, 3D-structure, dark field imaging

Abstract
X-ray computed-tomography (XCT) is a three-dimensional technique to reveal and quantify internal features and defects in materials. Conventional absorption-based contrast provides information on the attenuation of the X-ray beam intensity and is an invaluable tool in various domains, e.g. medicine and materials science. In the last decade however an important innovation in X-ray technology has emerged by the introduction of Talbot-Lau grating interferometry. This method provides three complementary image modalities in a single scan of the specimen: the absorption contrast (AC), the differential phase contrast (DPC), and the dark-field contrast (DFC). In this contribution we present results of a novel Talbot-Lau grating interferometry desktop µ-XCT-system which are compared to conventional high resolution XCT-results. In the first investigation we characterized polypropylene test specimens that are loaded in tensile testing until final failure. Lower grey levels near the fracture surface in the AC and DPC images indicate pores. Due to increased scattering in these regions DFC images provide high signal intensities, even though the defects are smaller than the spatial resolution. Furthermore we characterized crack-like defects in carbon fiber reinforced laminates that were subjected to impact forces up to 30 Joules using a high-velocity gas gun. Using DFC we are able to detect micro- cracks and delaminations in samples that were subject to low impact forces, whereas these defects are merely detectable using AC. In the third investigation we characterized an unfilled PP test specimen that was cyclically loaded in tensile testing until final failure.

1. Introduction

X-ray imaging methods and especially X-ray computed tomography (XCT) are essential techniques in order to reveal internal structures in materials. One of the most important and most recent innovations in X-ray technology has emerged by the introduction of the Talbot–Lau grating interferometry (TLGI). The additional use of a source grating to a TLGI enabled the introduction of this technique to polychromatic X-ray sources in 2006 [1,2,3]. In this set-up, the effect is based on the self-imaging of a grating whose period is a significant multiple of the wavelength. This method provides three complementary characteristics in a single scan of the specimen : Attenuation contrast (AC) due to absorption, Differential phase contrast (DPC) due to refraction and Dark-field contrast (DFC) due to scattering. AC provides information regarding the attenuation of the X-ray beam intensity through the specimen and it is thus equivalent to conventional X-ray imaging. DPC is related to the index of refraction and image contrast is thus achieved through the local deflection of the X-ray beam. DFC reflects the total amount of radiation scattered at small angles, e.g. caused by microscopic inhomogeneities in the sample such as particles, pores, and fibers. Depending on the micro-structure the scattering has a preferred direction perpendicular to the gratings delivering a dark-field signal that is varying with the orientation of the sample and its components [4,5].

Excerpt from ISBN 978-3-00-053387-7

Besides many applications in medicine and biology X-ray imaging with a tube based grating interferometer set-up has become a very valuable tool in materials research, too. For example grating-based X-ray imaging has been successfully applied to analyze the fibre structure of carbon and glass fibre reinforced polymers [3,4] and to obtain information on the micro-structure of cementitious materials [6].

In this contribution the damage in various polymeric samples after impact, tensile and vibrational testing using and a novel desktop micro-XCT system based on Talbot Lau Grating Interferometer was analysed and compared to a conventional absorption based X-ray CT system

2. Experimental

2.1. Samples and mechanical testing

For investigation 1 five carbon fiber reinforced (CFRP) laminate plates (20cm x 20cm) were impaired using a ball impact test for low impact energies (3 and 5 Joules) and a high-velocity gas gun for impact forces at 10, 15, and 20 Joules. The CFRP laminate were 3 mm in thickness, consisting of 15 layers and had a density of 311,3 g/m² (PREPREG C AGP193-P / 8552S / 38%) respectively. Samples for the TLGI-XCT investigations were cut out of the plates and showed a height of 5 cm and a width of 2 cm. For investigation 2 an unfilled polypropylene (PP) test specimen was investigated that was destroyed during tensile testing. The PP sample was scanned after failure. As third investigation (sample 3), an unfilled PP test specimen was characterized that was cyclically loaded in tensile testing until final failure. To guarantee, that the damage will occur in the region of interest, the sample was notched double sided. The test specimen was 5 cm in height and 1 cm in width. It was put under load for 434,631 cycles until breakage. The total duration of the procedure was 910 minutes which was performed in four intervals. The load (Fmin= 55 N and Fmax= 550 N) was applied at 8 Hz.

2.2. Talbot Lau grating interferometer XCT and high resolution absorption based XCT

Generally, a Talbot-Lau interferometer consists of two X-ray transmission gratings (G0 and G2), one phase grating (G1), in combination with a digital X-ray detector and an X-ray tube. G0 is moved sideways for phase stepping to measure the intensity modulation, the phase grating G1 is adjusted by rotation and tilting with respect to G2. The absorption grating G2 is mounted statically. Specimens were scanned at isometric voxel sizes using a Talbot-Lau grating interferometer XCT (Skyscan 1294). This new device was developed by Bruker microCT and it has a design energy of 30 keV. The main specifications are as follows:

- X-ray source with continuously adjustable 20-60 keV peak energy and a constant spot size with a diameter of 33 µm.
- 12-bit CCD-X-ray detector with 4000 x 2672 Pixels with Gadolinium oxysulfide as scintillator.
- The minimum voxel size is $(5.7\ \mu m)^3$ for 4000x2672 pixels.
- Motorized filter changer for energy selection with five filter positions.

Details of the novel TLGI-desktop XCT-system can be found in [4,5] and www.skyscan.be.

For all samples high-resolution reference scans at a voxel size between $(2\ \mu m)^3$ and $(5.7\ \mu m)^3$ were carried out using a sub-XCT system (GE Nanotom x|ray 180NF). The system has a nanofocus tube with a minimal focal spot size < 1 µm and a 2304x2304 pixel Hamamatsu detector. An overview of the measurement parameter used can be found in Table 1. XCT-data evaluation was done by Volume Graphics VG Studio Max 2.2. For minimum and maximum intensity projection calculation the tools of VG Studio Max were applied

Excerpt from ISBN 978-3-00-053387-7

Table 1. Scan parameters: voltage (U), voxel size, number of projections and filter.

Specimen Type	*U* (kV)	*Voxel size* $(\mu m)^3$	*Number of projections*	*filter*
Sample 1: CFRP (impact damage)				
TLGI-XCT (Skyscan)	35	22.8	720	0.25 Al
XCT (Nanotom)	60	2	1600	-
Sample 2: PP (tensile testing)				
TLGI-XCT (Skyscan)	35	22.8	720	0.25 Al
XCT (Nanotom)	55	3	1700	-
Sample 3: PP (Cylic testing)				
TLGI-XCT (Skyscan)	35	22.8	720	0.25 Al
XCT (Nanotom)	55	5.7	1700	-

3. Results and Discussion

3.1. Detection of damage after Impact

Figure 1 shows the TLGI- XCT scans of the CFRP samples after a 5 J impact. The data show the typical fibre bundle structure of CFRP-laminates, the concentric circles are ring artifacts. Even though the voxel size is ten times higher in the DFC images compared to XCT reference scans at $(2\ \mu m)^3$, micro-cracks can be detected in the DFC volume data. In contrast, micro-cracks are hardly visible in AC images measured at a voxel size of $(22.8\ \mu m)^3$ but clearly visible in the data set measured with $(2\ \mu m)^3$.

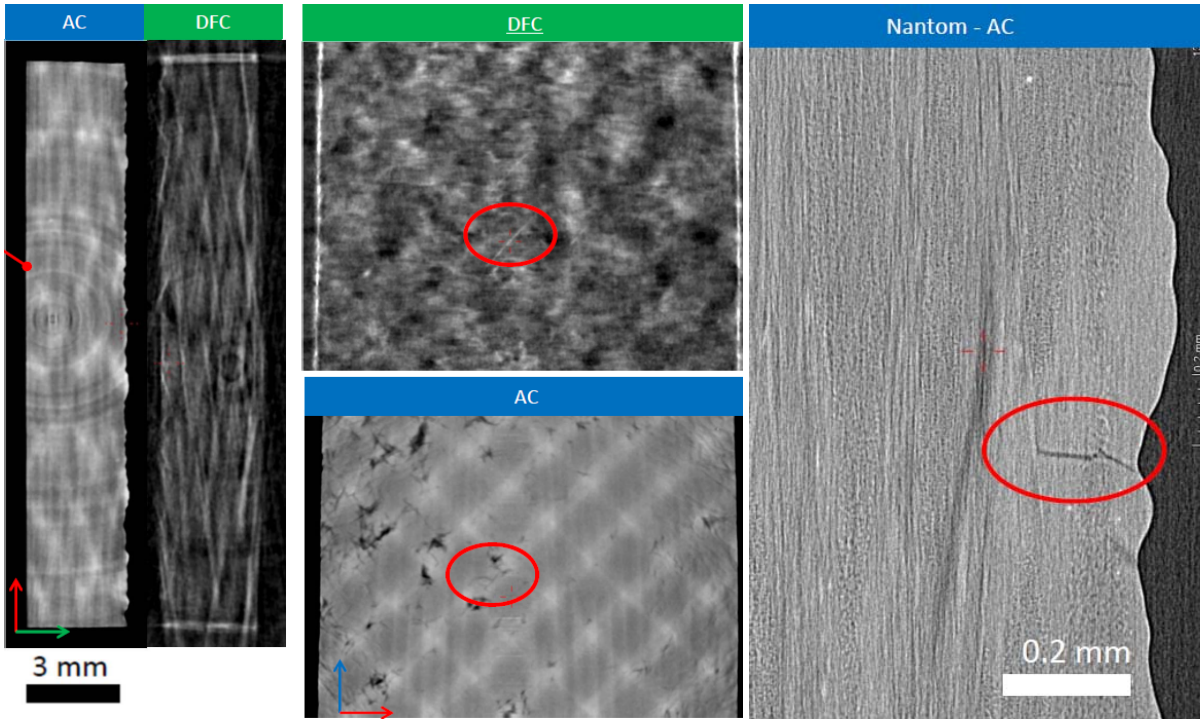

Figure 1. Transversal (left picture) and front view slices (pictures in the center) of a CFRP sample after a 5J impact measured with a TLGI-XCT (Skyscan 1294). The red arrow and ellipses mark the region of the impact. AC and DFC depict absorption and dark field contrast. The right picture shows a high resolution XCT slice measured with absorption contrast XCT (Nanotom) and $(2\ \mu m)^3$.

Excerpt from ISBN 978-3-00-053387-7

Figure 2 shows absorption contrast data (projection of minimum intensity) and dark field contrast data (projection of maximum intensity) of CFRP samples after impacts of 10 J, 15 J and 20 J. Cracks induced by the impact can be seen in both modalities. However, the DFC-data reveal much more details. The defects and cracks not detectable in the AC- data are precedently detected in the DFC-data. We quantified the amount of defects detectable in AC and DFC images as shown in Fig. 3. Maximum defect depth and width were defined as a visually detectable crack in the volume of the same sample. Fig. 3 clearly shows that the volume (depth and width) of the damage is always higher in the DFC than in the ACdata. This shows once again, that DFC can detect damage with a higher sensitivity than AC.

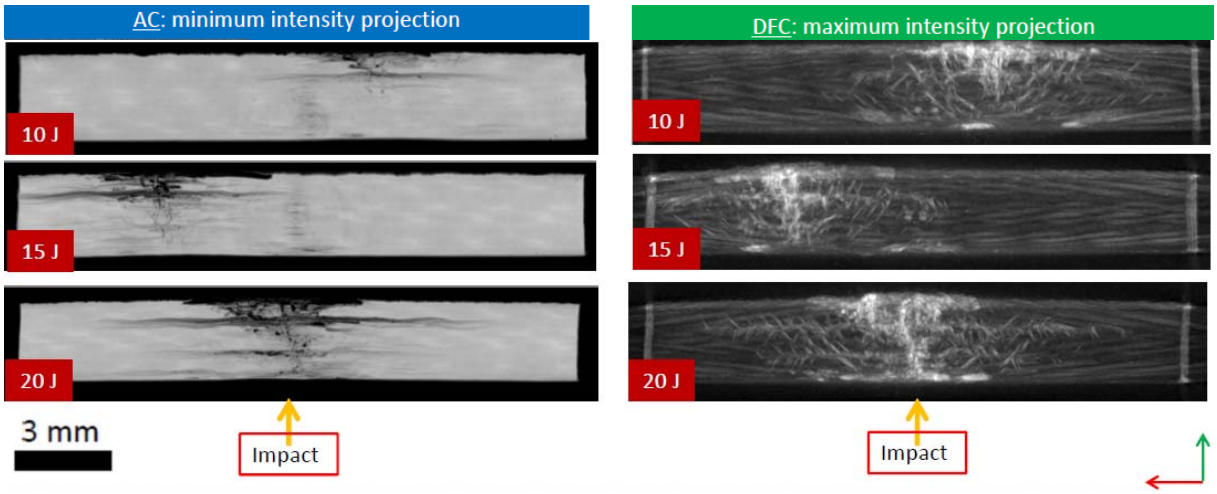

Figure 2. Absorption contrast data (projection of minimum intensity) and dark field contrast data (projection of maximum intensity) of CFRP samples after impacts of 10 J, 15 J and 20 J.

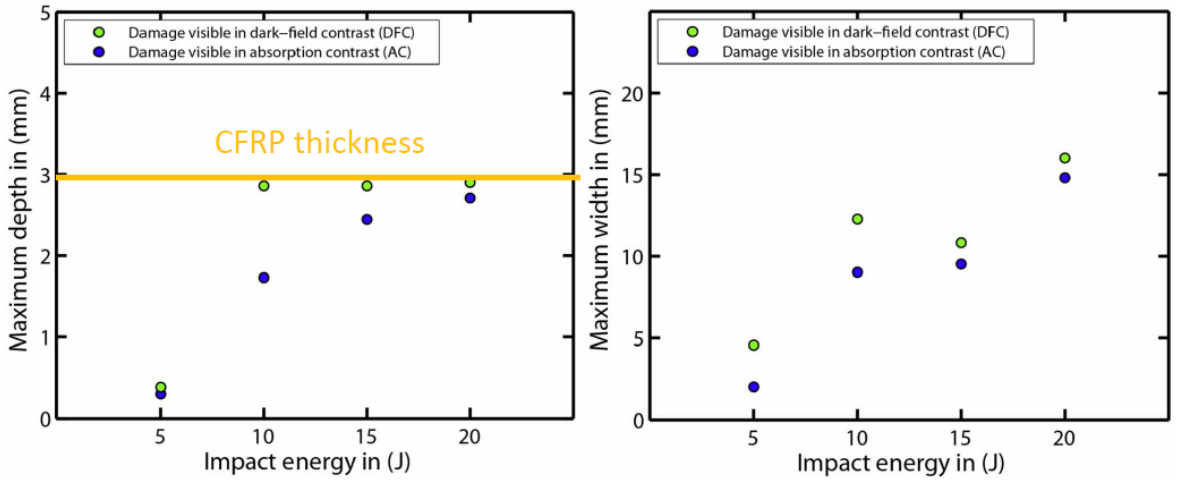

Figure 3. Quantitative evaluation of the TLGI-XCTdata. Defect depth in the axial plane determined from the AC (blue circles) and DFC (green circles) data (left picture) and defect width also determined from the AC and DFC data (right picture).

Excerpt from ISBN 978-3-00-053387-7

3.2. Detection of damage after tensile loading

In Figure 4 the AC, DPC and DFC images of a test specimen made of unfilled polypropylene that was destroyed during tensile testing are shown. In addition to the XCT-images obtained using the TLGI-µ-CT desktop device a detailed scan of the central part of the test specimens was obtained using a Nanotom 180NF system at a resolution of $(3\ \mu m)^3$. A lower grey level in the central part of the test specimens near the site of breakage in the AC (very left) and DPC (left) indicate the accumulation of defects like pores. The high signal intensity in the DFC image (right) is an additional indication of an increased scattering in this region due to small inhomogeneities like pores and cracks. These data-sets and in particular the high resolution ACdata clearly indicate the presence of defects induced during tensile testing [4].

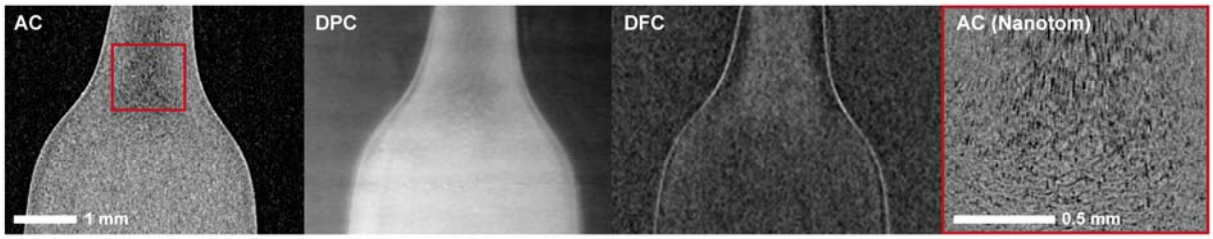

Figure 4. 3DCTdata of a polypropylene test specimen that was loaded in tensile testing until final failure in front view. A lower grey level in the central part of the test specimens near the site of breakage in the AC (left) and DPC indicate the accumulation of defects like pores. The right picture on the left was measured with the Nanotom µ-CT with a voxel size of $(3\ \mu m)^3$.

3.3. Detection of damage after cyclic loading

Finally an PP specimen that was cyclically loaded in interrupted tensile testing until final failure was investigated by TLGI- XCT. In total, the test specimen was loaded in four intervals. The first and second interval involved 172000 cycles respectively (time range: 0 – 360 min and 360 – 720 min respectively), the third interval comprised 86000 cycles (720 – 900 min). The sample broke after 4631 cycles in the last interval (900 – 910 min). Figure 5 shows AC and DFC images of the PP specimen in the original, unaffected state (Fig. 5a and b), after the first interval (Fig. 5c and d), after the second interval (Fig. 5e and f) and after the third interval (Fig. 5g and h). After the first loading interval, appearing cracks are obvious in the AC image represented by lower grey levels in the notch region. Those defects propagate during the subsequent intervals showing extensive accumulations of defects after the third interval. Accordingly, the dark field signal intensity increases during the different stages, showing spindle shaped structures in the maximum fatigue impact region near central notch in second and subsequent intervals (Fig. 5h).

Figure 6 shows the damage induced by the cycling in more detail. In the top image the high resolution AC data and in the lower image the DFC data are shown. In both images the cracks between the notches induced by cyclic loading are clearly detectable. In the ACdata individual cracks are visible and in the DFCmode the cracks and defects lead to a strong scattering and subsequently contributing to a strong signal. These data clearly show the possibility to characterize the damage after cycling loading by TLGI-XCT qualitatively and quantitatively. The results pertaining to quantitative evaluations would be published in forthcoming proceedings.

Excerpt from ISBN 978-3-00-053387-7

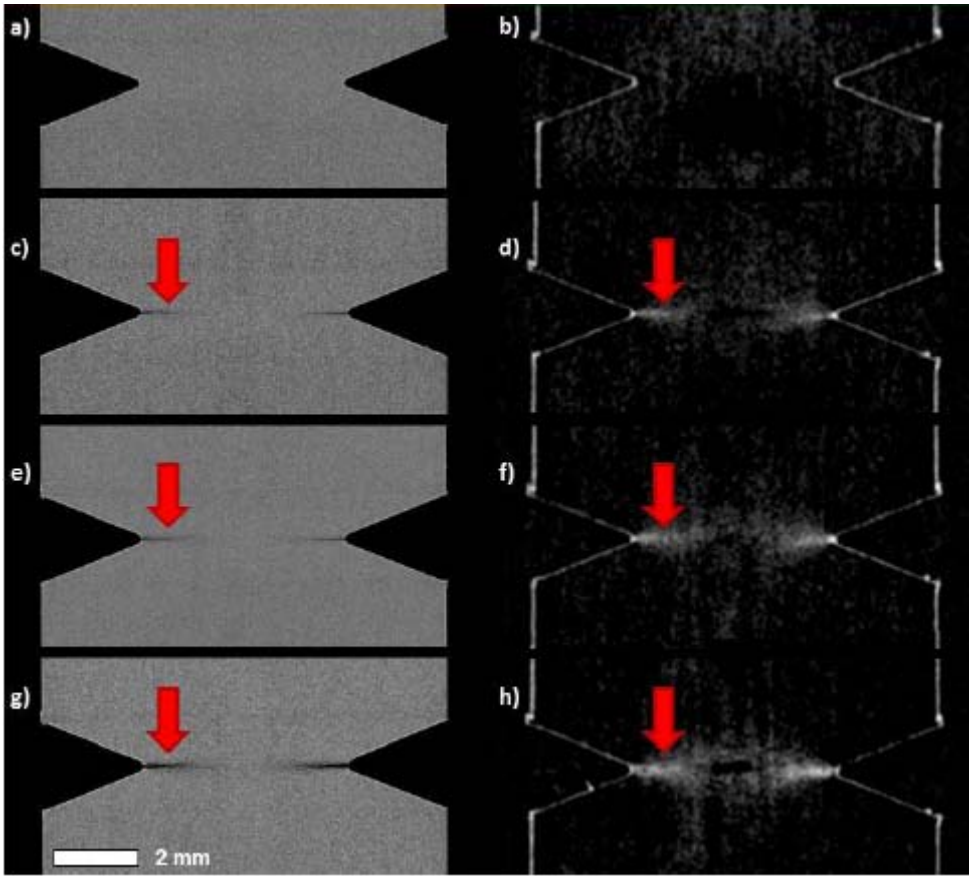

Figure 5. Frontal AC (left row) and DFC (right row) images of a PP test specimen subjected to interrupted cycling loading. Initial state: a) and b), after 172000 cycles: c) and d), after 344000 cycles: e) and f), and after 430000 cycles: g) and h). Red arrows indicate accumulations of defects in the notch region during loading.

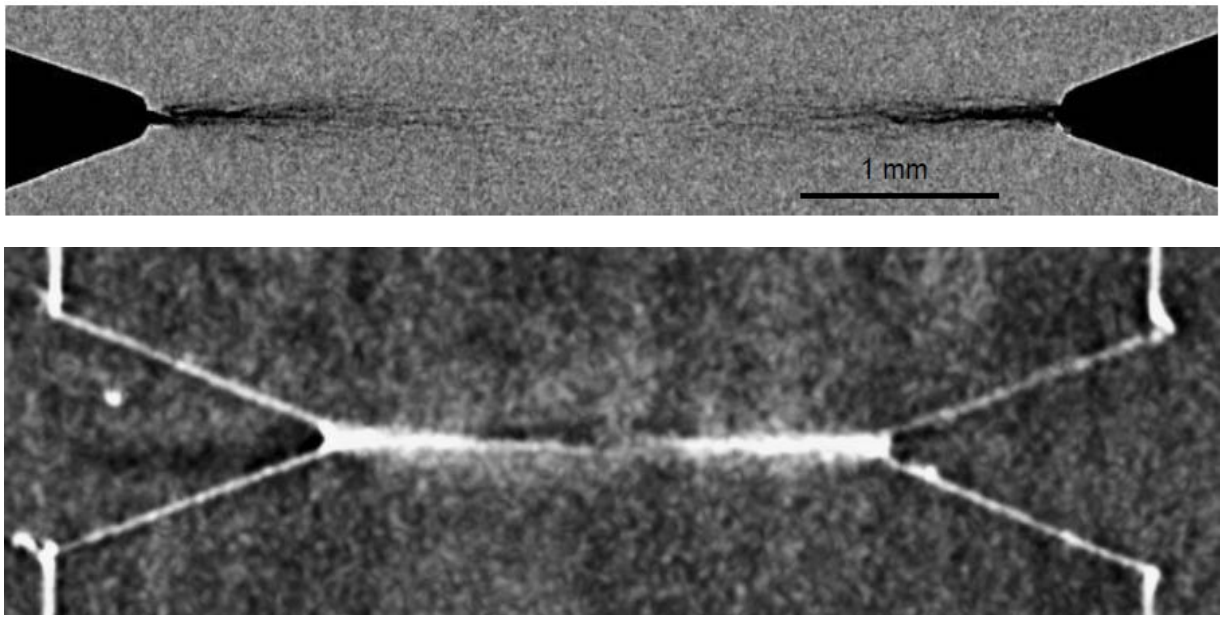

Figure 6. Frontal AC (top image) and DFC (lower image) images of a PP test specimen subjected to cycling loading after 430000 cycles. The AC-data were measured with $(5.7\ \mu m)^3$ and the DFC-data were measured with $(22.8\ \mu m)^3$.

Excerpt from ISBN 978-3-00-053387-7

4. Conclusions

We have reported on the application of a novel desktop micro-CT system based on TLGI for the characterization of the damage in polypropylene and carbon-fiber reinforced polymers after impact, tensile loading and cyclic loading. The data were compared with the results obtained using conventional absorption based high resolution XCT-device. The results of our investigation can be summarized as follows:

- Talbot-Lau grating interferometer XCT is a new innovative X-ray technology that expands imaging possibilities of standard XCT in material science by delivering information in form of dark-field contrast (DFC). Even though XCT imaging is a powerful tool for three-dimensional materials characterization, conventional absorption-based methods are not able to detect defects that are below the physical resolution of the respective system. The introduction of DFC imaging helps to overcome this limitation.
- We have shown that DFC allows the identification of cracks in CFRP laminates, which are smaller than the spatial resolution of the reference XCT system. Sample size is a major limiting factor in high-resolution XCT, however DFC imaging allows the identification of (micro-) cracks in relatively large samples with at a relatively low voxel size, in our case at $(22.8\ \mu m)^3$. Moreover, we were able to show that the amount of detectable defects in DFC images exceeded the information on defect distribution in AC images.
- We have demonstrated the possibilities of the detection of damage in polypropylene samples after tensile testing by TLGI-XCT. The occurrence of defects lead to lower grey values in the ACand DPCdata and to higher grey values due to scattering in the DFCdata.
- Finally we have investigated the damage in a polypropylene sample after cyclic loading by AC and DFC. In both modalities cracks between the notches induced by the cyclic loading are clearly detectable, in the ACdata individual cracks are visible and the in the DFC-mode the cracks and defects lead to a strong scattering and subsequently to a strong signal. A qualitative and also quantitative characterization by TLGI-XCT is possible.

Acknowledgments

The work was financed by the K-Project ZPT+, supported by the COMET program of FFG and by the federal government of Upper Austria and Styria and by the EFRE IWB2020 program within the project MICI - Multimodale und in-situ Charakterisierungsverfahren für inhomogene Werkstoffe.

References

[1] C. David, B. Nöhammer, H.H. Solak, and E. Ziegler, Differential x-ray phase contrast imaging using a shearing interferometer, *Appl Phys Lett,* 81:3287-3297, 2002.

[2] F. Pfeiffer, T. Weitkamp, O. Bunk, and C. David, Phase retrieval and differential phase-contrast imaging with low-brilliance X-ray sources, *Nature Physics,* 2:258–267, 2006.

[3] V. Revol, B. Plank, R. Kaufmann, J. Kastner, Ch. Kottler, and A. Neels, Laminate fibre structure characterisation of carbon fibre-reinforced polymers by X-ray scatter dark field imaging with a grating interferometer, *NDT&E International,* 58:64–71, 2013.

[4] J. Kastner, S. Senck, C. Gusenbauer, B. Plank, C. Hannesschläger, H. Zauner, C. Heinzl and A. Sasov, Three-dimensional characterization of fibre-reinforced polymers using a Talbot-Lau grating interferometer µ-CT und data fusion methods, *Proceedings Conference on X-ray and Neutron Phase Imaging with Gratings XNPIG2015, Bethesda, USA*, September 8.-11 2015.

[5] C. Gusenbauer, E. Leiss-Holzinger, S. Senck, K. Mathmann, J. Kastner, and S. Hunger. Characterization of medical and biological samples with a Talbot–Lau grating interferometer µXCT in comparison to reference methods, *Case Studies in NDT&E International*, 1:1–9, 2016.

Excerpt from ISBN 978-3-00-053387-7

[6] F. Yang, F. Prade, M. Griffa, I. Jerjen, C. D. Bella, J. Herzen, A. Sara-pata, F. Pfeiffer, and P. Lura, Dark-field x-ray imaging of unsaturated water transport in porous materials, *Appl. Phys. Lett.,* 105: 154105-154111, 2014.

Excerpt from ISBN 978-3-00-053387-7